Hindawi Publishing Corporation
International Journal of Photoenergy
Volume 2014, Article ID 503516, 9 pages
http://dx.doi.org/10.1155/2014/503516

Research Article

Role of Platinum Deposited on TiO_2 in Photocatalytic Methanol Oxidation and Dehydrogenation Reactions

Luma M. Ahmed,[1] Irina Ivanova,[2] Falah H. Hussein,[3] and Detlef W. Bahnemann[2]

[1] *Chemistry Department, College of Science, Karbala University, 56001 Karbala, Iraq*
[2] *Institut für Technische Chemie, Leibniz Universität Hannover, Callin Strasse 3, 30167 Hannover, Germany*
[3] *Chemistry Department, College of Science, University of Babylon, 51002 Hilla, Iraq*

Correspondence should be addressed to Falah H. Hussein; abohasan_hilla@yahoo.com

Received 30 November 2013; Revised 4 January 2014; Accepted 5 January 2014; Published 20 February 2014

Academic Editor: Jiaguo Yu

Titania modified nanoparticles have been prepared by the photodeposition method employing platinum particles on the commercially available titanium dioxide (Hombikat UV 100). The properties of the prepared photocatalysts were investigated by means of the Fourier transform infrared spectroscopy (FTIR), X-ray diffraction (XRD), atomic force microscopy (AFM), and UV-visible diffuse spectrophotometry (UV-Vis). XRD was employed to determine the crystallographic phase and particle size of both bare and platinised titanium dioxide. The results indicated that the particle size was decreased with the increasing of platinum loading. AFM analysis showed that one particle consists of about 9 to 11 crystals. UV-vis absorbance analysis showed that the absorption edge shifted to longer wavelength for 0.5% Pt loading compared with bare titanium dioxide. The photocatalytic activity of pure and Pt-loaded TiO_2 was investigated employing the photocatalytic oxidation and dehydrogenation of methanol. The results of the photocatalytic activity indicate that the platinized titanium dioxide samples are always more active than the corresponding bare TiO_2 for both methanol oxidation and dehydrogenation processes. The loading with various platinum amounts resulted in a significant improvement of the photocatalytic activity of TiO_2. This beneficial effect was attributed to an increased separation of the photogenerated electron-hole charge carriers.

1. Introduction

Titanium dioxide is regarded to be one of the most common photocatalysts, having a wide range of properties, such as a strong resistance to chemical and photocorrosion, strong oxidation capability, low operational temperature, low-cost, being and nontoxic [1]. These properties make TiO_2 an attractive candidate for its utilization as a photocatalyst in the photocatalytic processes. TiO_2 has been extensively studied and demonstrated to be suitable for numerous applications such as, destruction of microorganisms [2–5], inactivation of cancer cells [6, 7], protection of the skin from the sun [8–11], photocatalytic water splitting to produce hydrogen gas [12–14], manufacture of some drug types [15–17], degradation of toxic organic pollutants in water [18–20], and self-cleaning of glass and ceramic surfaces [21]. Even though TiO_2 is the most used semiconductor material, it exhibits some disadvantages, such as low surface area and fast recombination rate between the photogenerated charge carriers and the maximum absorption in the ultraviolet light region.

Different attempts have been performed to improve the efficiency of TiO_2 depressing the recombination process of the photoelectron-hole pairs. Some of them include the modification of TiO_2 surface with other semiconductors to alter the charge-transfer properties between TiO_2 and the surrounding environment [22, 23], sensitizing TiO_2 with colored inorganic or organic compounds improving its optical absorption in the visible light region [24–28], bulk modification by cation and anion doping [29–38], and fabrication of TiO_2 surface from polyhedral to produce hallow TiO_2

[39, 40]. TiO_2 nanoparticles are considered to be more active photocatalysts as compared with the bulk powder. The ratio of surface area to volume of nanoparticles has a significant effect on nanoparticles properties. This leads to a higher chemical activity and loss of magnetism and dispersibility [41].

This work was focused on the characterization of the prepared Pt-loaded TiO_2 (Hombikat UV 100) samples. Moreover, the photocatalytic oxidation and photocatalytic dehydrogenation of methanol have been studied employing both the bare and Pt-loaded TiO_2 in the O_2 and N_2 atmosphere. The methanal formation was determined using Nash method at a wavelength of 412 nm.

2. Materials and Methods

A known weight (2 g) of TiO_2 (Hombikat UV 100, Sachtleben, Germany) was suspended under continuous stirring at 250 rpm in a solution containing 40 cm^3 of 40% aqueous methanal (Chemanol), 10 cm^3 of methanol (Hayman), and the appropriate volume of hexachloroplatinic acid (Riedel-De-Haen AG) dissolved in HCl. The reaction mixture was maintained at 303 K, purged with nitrogen gas (20 cm^3/min) and irradiated by UV-A light employing Philips Hg lamp (90 W) with the light intensity of 3.49 mW/cm^2 (Efbe-Schon 6 lamps) for 4 h. This period of irradiation time was found to be the most sufficient time for the complete photodeposition process of metallic platinum. The concentration of platinum was monitoring by the atomic absorption spectroscopy (Shimadzu-AA-6300, Japan). The milky white suspension turns to the pale grey colour with the deposition of Pt. The suspension solution was filtered and washed by absolute methanol, throwing in a desecrater overnight. At the end the product was dried in an oven at 100°C for 2 h [31, 32]. Band gap energies of bare and Pt (0.5)-loaded on TiO_2 surface were determined, via the measurement of reflectance data R by (Cary 100 Scan) UV-visible spectrophotometer system. It is equipped, with using a Labsphere integrating sphere diffuse reflectance accessory for diffuse reflectance spectra over a range of 300–500 nm by employing $BaSO_4$ as reference material.

In all photocatalytic experiments, 100 cm^3 of 40 mM aqueous methanol solution (HPLC grade, Sd fine-CHEM limited) was mixed with certain weight of bare TiO_2 or platinized TiO_2 and was suspended using a magnetic stirrer at 500 rpm. At different time of intervals 2.5 cm^3 of reaction mixture was collected in a plastic test tube and centrifuged (4000 rpm, 15 minutes) in an 800 B centrifuge. The supernatant solution was carefully removed by a syringe to a new plastic test tube and centrifuged again to remove the fine particles of bare TiO_2 or platinized TiO_2. The concentration of formed methanal was determined spectrophotometrically at 412 nm following Nash method [42, 43] using UV-visible spectrophotometer (T80+, PG Instruments Limited, England).

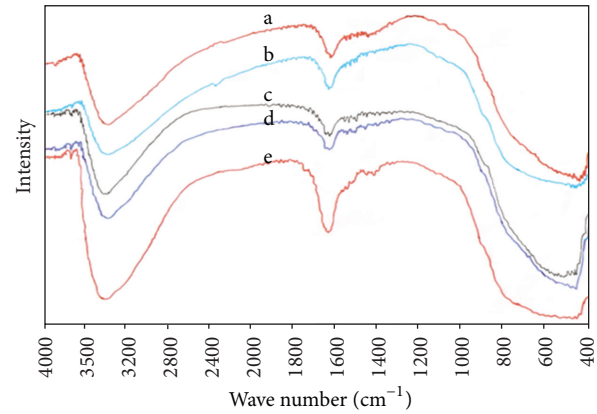

Figure 1: FT-IR spectra for bare and different percentages of Pt-loaded on TiO_2, at (a) bare TiO_2, (b) Pt (0.25)/TiO_2, (c) Pt (0.50)/TiO_2, (d) Pt (0.75)/TiO_2, and (e) Pt (1.00)/TiO_2.

3. Results and Discussion

3.1. Characterisation of Bare and Platinized TiO_2

3.1.1. FTIR Analysis. The Fourier transform infrared spectra of bare and platinized TiO_2 are depicted in Figure 1. The illustrated peaks at 3350–3450 cm^{-1} correspond to the stretching vibration mode of O–H bonds of free water molecules and at 1620–1630 cm^{-1} correspond to the bending vibration mode of O–H bond of chemisorbed water molecules. The absorption intensity of surface O–H groups in TiO_2 is regularly increased with the increasing of the percentage of metals content. These findings are in a good agreement with the literature data [44–46]. The broad intense band below 1200 cm^{-1} is due to Ti–O–Ti bridging stretching mode in the crystal. This peak appeared as unsymmetrical valley with the increasing of metal loading (or content) on TiO_2 exhibiting a maximum at 580 cm^{-1}. This change is related to the formation of Ti–O–M vibrations [47, 48]. The intense bands at 3621, 3645, and 3696 cm^{-1} in all spectra are attributed to the characteristic tetrahedral coordinated vacancies of $_4Ti^{4+}$–OH besides two bands at 3765 and 3840 cm^{-1}. These revealed that the octahedral vacancies designated as $_6Ti^{3+}$–OH are found. In the presence of metal loaded on TiO_2 the peaks of $_6Ti^{3+}$–OH are not observed. This is because the metal acts as an electron trapper, mainly preventing the formation of Ti^{3+}–OH species [49]:

$$Ti^{4+}\text{–OH} + e^- \longrightarrow Ti^{3+}\text{–OH} \quad (1)$$

$$M + e^- \longrightarrow M^- \quad (2)$$

3.1.2. XRD Analysis. The XRD patterns of different TiO_2 samples (bare and platinum loaded) are shown in Figure 2. The mean crystallite size (L) of samples was calculated by Scherrer's equation (3) and the crystallite size ($\acute{L}$) of samples can be estimated from plotting the modified Scherrer's

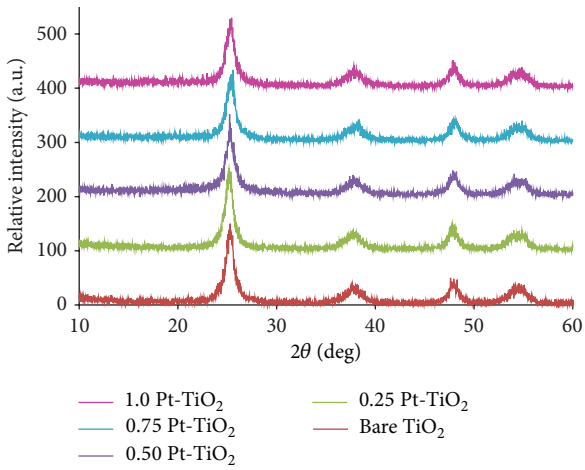

Figure 2: XRD patterns of bare and different percentage of Pt loaded on TiO_2 surface.

formula (4) [50] as shown in Figure 3. The corresponding values are listed in Table 1:

$$L = \frac{k\lambda}{\beta \cos\theta}, \tag{3}$$

$$\ln\beta = \ln\left(\frac{k\lambda}{\acute{L}}\right) + \ln\left(\frac{1}{\cos\theta}\right). \tag{4}$$

In (3) and (4), k is Scherer's constant depending on shape of particles (0.94), λ is the wavelength of the X-ray radiation (0.15418 nm for CuK_α), β is the full width of half maximum (FWHM) intensity (in degree which converted to radian), and θ is the diffraction (Bragg) angle [50, 51].

No peak was observed for Pt (0.25 wt%)/TiO_2 sample at $\theta = 46.5^\circ$. This result is in good agreement with the previous findings [52]. However, $\theta = 46.6^\circ$ which is related to Pt appeared very weak band with Pt (0.5%) loading and increased for Pt (1.0%) as shown in Figure 2. The mean crystallite size of both bare and platinized TiO_2 decreased from 11.487 nm to 9.355 nm, respectively. The crystallite size of bare TiO_2 was found to be equal to 10.132 nm. This value was decreased with the increasing of Pt content on TiO_2. The decreasing of the mean particle size of platinized TiO_2 is attributed to the location and incorporation of Pt(IV) with Ti(III) in TiO_2 lattice. Moreover, the ionic radius of Pt(IV) (0.63 Å) is relatively smaller than that of Ti(III) (0.67 Å) [53, 54].

3.1.3. AFM Analysis. Figure 4 shows the three-dimensional AFM images of bare and Pt-loaded TiO_2 surface which were used to measure the particle sizes. AFM images indicate that the shapes of both bare and platinized TiO_2 are spherical. The results summarized in Tables 1 and 2 indicate that the particle sizes for all samples are found to be bigger than the values found for crystallite size. This indicates that each particle consists of several crystals (polycrystals) [55]. The values of crystal size and particle size for bare TiO_2 are more than those values for metalized TiO_2. This is related to the

Table 1: Mean crystallite sizes and crystallite sizes of bare TiO_2 and Pt-loaded on TiO_2.

Crystal components	Pt %	Mean crystallite sizes (L)/nm	Crystallite sizes ($\acute{L}$)/nm
TiO_2 Hombikat (UV 100)	0.000	11.487	10.132
Pt-TiO_2	0.250	10.799	10.021
Pt-TiO_2	0.500	9.355	9.503
Pt-TiO_2	0.750	10.221	9.589
Pt-TiO_2	1.000	10.475	8.262

increasing of the number of located of Pt^{4+} ions in TiO_2 lattice, which depresses the growth of TiO_2 Hombikate (UV 100) nanocrystals [54]. The results show that each particle consists of about 9 to 11 crystals, according to the results obtained from the calculation of Crystallinity Index values by employing the following equation [56]:

$$\text{Crystallinity Index} = \frac{D_p}{L \text{ or } \left(\acute{L}\right)}, \tag{5}$$

where D_p is the particle size which is measured by AFM analysis and L and $\acute{L}$ are the corresponding mean crystallite size and the crystallite size calculated by the Scherrer equation and the modified Scherrer equation employing XRD data, respectively.

The maximum value of average Crystallinity index for Pt (0.5)/TiO_2 is found to be 8.168. That referred to the suppression of the crystal defects number through decreasing the amorphous phase present in TiO_2 and overall enhancing the photocatalytic activity of TiO_2 [57].

3.1.4. UV-Visible Diffuse Reflectance Spectra. The UV-vis absorbance spectra of the bare TiO_2 and platinized TiO_2 (0.5% Pt) powders were also measured to confirm the Pt-loading trend and to measure the effect of Pt loading. The results from UV-visible reflectance spectra as plotted in Figure 5 clearly show the shift of absorption edge towards longer wavelength for platinized TiO_2. These results indicate that the excitation of metalized TiO_2 occurs with the narrowing and red shift of the band gap energy (E_g) peak [58]. These results were subsequently agreed with the increasing of the average Crystallinity Index [57].

3.2. Effect of the Metal Loading on Photocatalytic Activity of Methanol Solution. The photocatalytic activity of the platinized titanium dioxide was first increased with the increasing of the metal loading until a maximum was reached with the following decrease in the activity. Figures 6 and 7 show the results obtained with the samples containing different amount of platinum. The highest photocatalytic activity was observed with the Pt loading of 0.5 wt%. This loading percentage may give the most efficient separation of photogenerated electron-hole pairs [59]. The presence of Pt on the TiO_2 surface leads to an increase of the surface barrier and the space charge region becomes narrower. As a result of

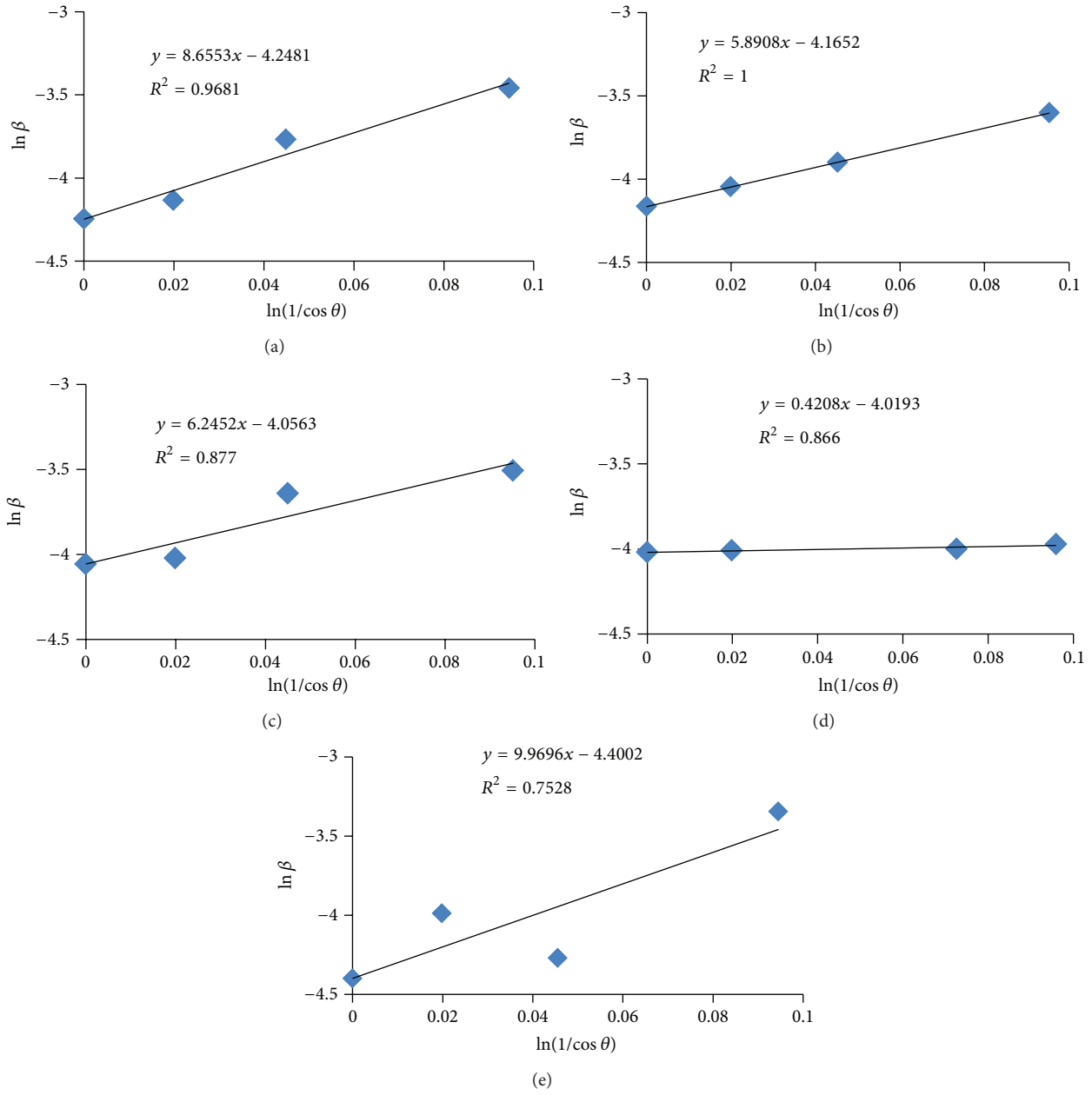

Figure 3: Modified Scherrer equation plot of (a) bare TiO_2, (b) 0.25% Pt loaded on TiO_2, (c) 0.50% Pt loaded on TiO_2, (d) 0.75% Pt loaded on TiO_2, and (e) 1.00% Pt loaded on TiO_2.

Table 2: Particle size measured by AFM and Crystallinity values of bare TiO_2 and platinized TiO_2.

Samples	Particle size/nm	*Crystallinity Index	**Crystallinity Index	Average Crystallinity Index
TiO_2	80.940	7.046	7.988	7.517
Pt(0.25)/TiO_2	63.600	5.889	6.346	6.117
Pt(0.50)/TiO_2	77.020	8.233	8.104	8.168
Pt(0.75)/TiO_2	54.890	5.370	5.724	5.547
Pt(1.00)/TiO_2	73.130	6.981	8.851	7.916

*Crystallinity Index calculated by divided particle size on mean crystallite size and **Crystallinity Index calculated by divided particle size on crystallite size.

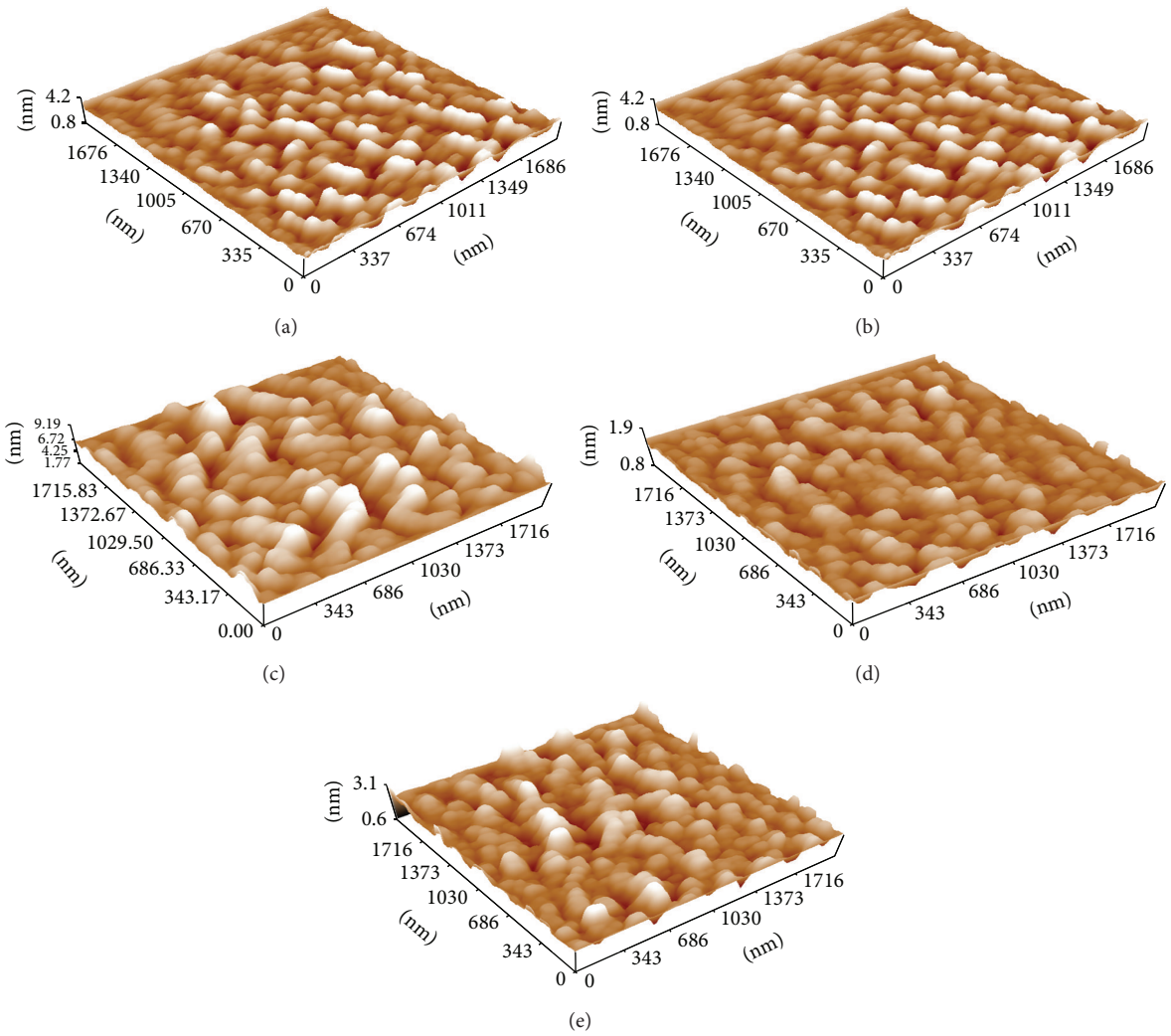

FIGURE 4: Three-dimensional AFM image of (a) bare TiO_2, (b) 0.25% Pt loaded on TiO_2, (c) 0.50% Pt loaded on TiO_2, (d) 0.75% Pt loaded on TiO_2, and (e) 1.00% Pt-loaded on TiO_2.

the metal loading the space charge region becomes narrower leading to an increase of the efficiency of the electron-hole separation [60] and formation of the Schottky barrier by the electron transfer from the conduction band of TiO_2 to the conduction band of Pt. Thereby the recombination process is suppressed according to the following equations [31, 32, 61]:

$$\mathrm{Pt/TiO_2} + h\nu \longrightarrow \mathrm{h^+_{VB}} + \mathrm{e^-_{CB}} \quad (6)$$

$$\mathrm{Pt}_n + \mathrm{e^-_{CB}} \longrightarrow \mathrm{Pt^-}_n \quad (7)$$

$$\mathrm{O_2} + \mathrm{Pt^-}_n \longrightarrow \mathrm{O_2^{-\bullet}} + \mathrm{Pt}_n. \quad (8)$$

Platinum acts as electron scavenger hindering the recombination of the charge carriers and ultimately exhibiting the enhancement of the photoreactivity as shown in the following equation [31, 32, 62, 63]:

$$\mathrm{Pt^-}_n + \mathrm{h^+_{VB}} \longrightarrow \mathrm{Pt}_n. \quad (9)$$

However, when the percentage of the metal reached maximum, the additional amount leads to making the space charge layer very narrow. As a result the penetration depth of light exceeds the space charge layer. The recombination of the electron-hole pairs will be favorable and the photocatalytic activity will be reduced [60]. Moreover, the presence of metal on the TiO_2 surface reduces the number of the surface hydroxyl groups leading to the reduction of the photoreactivity [64]. This means that the metal on the TiO_2 surface acts both as an efficient trap site and as a recombination center at the same time [65]. Hence the rate of the methanal (HCHO) formation will be slower while the conversion of methanal to formic acid (HCOOH) is a faster process. On the other hand, with the increasing of the metal amount, TiO_2 samples will become more grey in color. Thus, the changed optical properties of the samples could lead to the screening of the light towards the TiO_2 and suppression of the electrons excitation to the conduction band [31, 66].

Two mechanisms for the photocatalytic oxidation (in the presence of O_2) and photocatalytic dehydrogenation (in the presence of N_2) of methanol with Pt (0.5)/TiO_2 are suggested as shown in Scheme 1. The scheme shows the differences

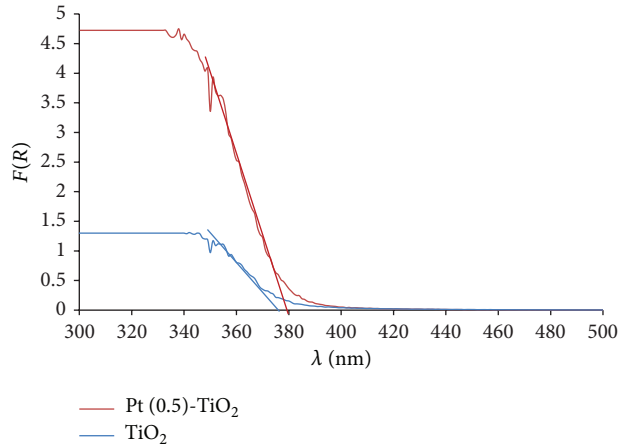

Figure 5: UV-visible diffuse reflectance spectra of bare and Pt-loaded on TiO_2 surface.

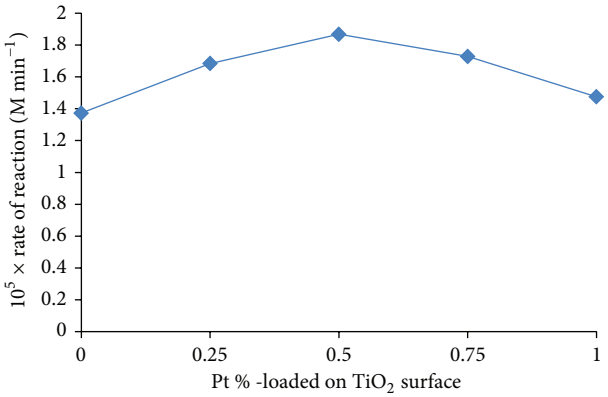

Figure 6: Rate of methanal formation as function of bare and different percentage of Pt on TiO_2 surface, under purged O_2.

between the mechanism of photooxidation and photodehydrogenation of methanol on platinized titanium dioxide. The formation of $CaCO_3$ in photooxidation process was indicated by passing the outlet gas in $Ca(OH)_2$ solution. However, no CO_2 formation was indicated in photodehydrogenation of methanol.

Differences in experimental conditions, such as, experimental equipment, type of photocatalyst, position of band edges of semiconductor compared to redox potential of $O_2/O_2^{-\bullet}$ and $^{-}OH/^{\bullet}OH$, and type and concentration of organic pollutant, cause difficulties in the comparison of photocatalytic activity of different materials. Xiang et al. [67] measured the formation rates of hydroxyl free radical for various semiconductor photocatalysts at the same experimental conditions. They discussed the difference of rates formation of hydroxyl free radical on various semiconductors. In another study Xiang et al. [68] showed that hydroxyl radicals are one of active species and indeed participate in photocatalytic reactions. They also found that the photocatalytic activity of Ag-TiO_2 exceeds that of P25 by a factor of more than 2. Our results are in good agreement with these findings.

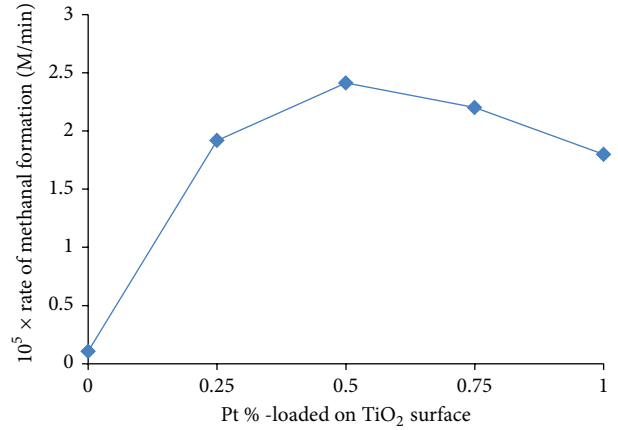

Figure 7: Rate of methanal formation as function of bare and different percentage of Pt on TiO_2 surface, under purged N_2.

The different yields that are suggested in the two mechanisms are HCOH and H_2O in the absence of oxygen (photocatalytic dehydrogenation of methanol) and HCOOH in the presence of oxygen (photocatalytic oxidation of methanol). The pH of the reaction suspension after one hour of irradiation was found 6.93 in dehydrogenation process while it was 4.82 in photooxidation process. This indicates the further oxidation of the formed formaldehyde to formic acid.

4. Conclusions

This study is focused on the elucidation of the mechanism of the methanol formation by the photocatalytic oxidation and/or photocatalytic dehydrogenation of aqueous methanol solution with bare and platinized TiO_2. The main conclusions can be summarized as follows.

(1) The FT-IR spectra show that the peaks at 3450 cm^{-1} and 1630 cm^{-1} related to the surface O–H groups of TiO_2 are increased with the increasing of the platinum amount loaded on TiO_2 surface. The intense bands at 3621, 3645, and 3696 cm^{-1} have been observed in all spectra which are characteristics for the tetrahedral coordinated vacancies designated as $_4Ti^{4+}$–OH. Additionally, a disappearance of two bands at 3765 and 3840 cm^{-1} attributed to $_6Ti^{3+}$–OH has been observed as well.

(2) The XRD data have been used to calculate the crystallite size of the bare and Pt-loaded TiO_2. The values obtained for the crystallite size of the bare TiO_2showed a decrease with the increasing of platinum amount on TiO_2.

(3) AFM images indicate that the shapes of both bare and platinized TiO_2 are spherical.

(4) One particle consists of about 9 to 11 crystals.

(5) In photoreaction, no reaction occurred with using bare TiO_2 under inert gas (N_2); however, in the presence of metal, the photoreaction occurred; that is, the existence of the metal substituted the needed

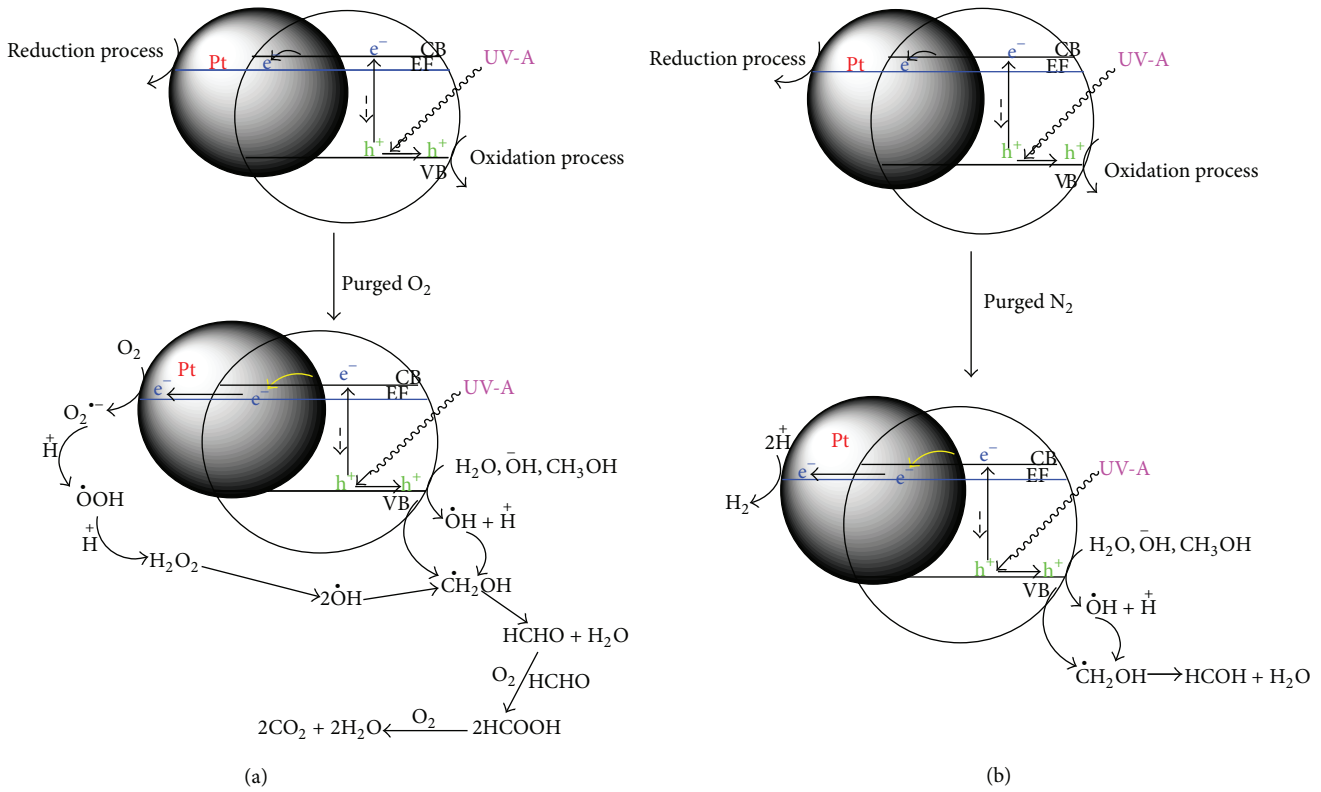

Scheme 1: General mechanism of photocatalytic of methanol with platinized TiO_2 under (a) passing O_2 and (b) passing N_2.

for the O_2. In the existence of O_2 the reaction was carried on to form formic acid as a result of further oxidation of methanol while, in the absence of the O_2, dehydrogenation of methanol occurred, and no further photooxidation occurred.

Conflict of Interests

The authors declare that there is no conflict of interests regarding the publication of this paper.

References

[1] H. Yang, S. Zhu, and N. Pan, "Studying the mechanisms of titanium dioxide as ultraviolet-blocking additive for films and fabrics by an improved scheme," *Journal of Applied Polymer Science*, vol. 92, no. 5, pp. 3201–3210, 2004.

[2] J. A. Ibáñez, M. I. Litter, and R. A. Pizarro, "Photocatalytic bactericidal effect of TiO_2 on *Enterobacter cloacae*. Comparative study with other Gram (−) bacteria," *Journal of Photochemistry and Photobiology A*, vol. 157, no. 1, pp. 81–85, 2003.

[3] M. Haghi, M. Hekmatafshar, B. Mohammad Janipour et al., "Antibacterial effect of TiO_2 nanoparticles on pathogenic strain of *E. coli*," *International Journal of Advanced Biotechnology and Research*, vol. 3, no. 3, pp. 621–624, 2012.

[4] L. Zhang, J. Yan, M. Zhou, and Y. Liu, "Photocatalytic inactivation of bacteria by TiO_2-based compounds under simulated sunlight irradiation," *International Journal of Material Science*, vol. 2, no. 2, pp. 43–46, 2012.

[5] R. Liu, H. Wu, R. Yeh, C. Lee, and Y. Hung, "Synthesis and bactericidal ability of TiO_2 and Ag-TiO_2 prepared by coprecipitation method," *International Journal of Photoenergy*, vol. 2012, Article ID 640487, 7 pages, 2012.

[6] A.-P. Zhang and Y.-P. Sun, "Photocatalytic killing effect of TiO_2 nanoparticles on Ls-174-t human colon carcinoma cells," *World Journal of Gastroenterology*, vol. 10, no. 21, pp. 3191–3193, 2004.

[7] T. Sungkaworn, W. Triampo, P. Nalakarn, I. Tang, Y. Lenburg, and P. Picha, "The Effects of TiO_2 nanoparticales on tumor cell colonies: fractal dimension and morphological properties," *International Journal of Biological and Life Sciences*, vol. 2, no. 1, pp. 67–74, 2007.

[8] A. Popov, *TiO_2 Nanoparticles as Uv Protectors in Skin*, Oulun Yliopisto, Oulu, Finland, 2008.

[9] C.-C. Lin and W.-J. Lin, "Sun protection factor analysis of sunscreens containing titanium dioxide nanoparticles," *Journal of Food and Drug Analysis*, vol. 19, no. 1, pp. 1–8, 2011.

[10] S. Singh and A. pal, "Review: emergence of novel nanoparticles as Uv absorber in sunscreen and their application," *International Journal of Pharmaceutical Research & Development*, vol. 4, no. 3, pp. 207–216, 2012.

[11] A. P. Popov, A. V. Zvyagin, J. Lademann et al., "Designing inorganic light-protective skin nanotechnology products," *Journal of Biomedical Nanotechnology*, vol. 6, no. 5, pp. 432–451, 2010.

[12] E. Selli, G. L. Chiarello, E. Quartarone, P. Mustarelli, I. Rossetti, and L. Forni, "A photocatalytic water splitting device for separate hydrogen and oxygen evolution," *Chemical Communications*, no. 47, pp. 5022–5024, 2007.

[13] J. Oudenhoven, F. Scheijen, and M. Wollfs, "Fundamental of photocatalytic water splitting by visible light," *Chemistry of Catalytic System 2: Photocatalysis*, pp. 1–22, 2004.

[14] A. Fujishima and K. Honda, "Electrochemical photolysis of water at a semiconductor electrode," *Nature*, vol. 238, no. 5358, pp. 37–38, 1972.

[15] M. Del Arco, S. Gutiérrez, C. Martín, V. Rives, and J. Rocha, "Synthesis and characterization of layered double hydroxides (LDH) intercalated with non-steroidal anti-inflammatory drugs (NSAID)," *Journal of Solid State Chemistry*, vol. 177, no. 11, pp. 3954–3962, 2004.

[16] H. Zhang, K. Zou, S. Guo, and X. Duan, "Nanostructural drug-inorganic clay composites: structure, thermal property and in vitro release of captopril-intercalated Mg-Al-layered double hydroxides," *Journal of Solid State Chemistry*, vol. 179, no. 6, pp. 1792–1801, 2006.

[17] S.-J. Xia, Z.-M. Ni, Q. Xu, B.-X. Hu, and J. Hu, "Layered double hydroxides as supports for intercalation and sustained release of antihypertensive drugs," *Journal of Solid State Chemistry*, vol. 181, no. 10, pp. 2610–2619, 2008.

[18] F. Hussein, "Comparison between solar and artificial photocatalytic decolorization of textile industrial wastewater," *International Journal of Photoenergy*, vol. 2012, Article ID 793648, 10 pages, 2012.

[19] S. Devipriya, S. Yesodharan, and E. Yesodharan, "Solar photocatalytic removal of chemical and bacterial pollutants from water using Pt/TiO_2-coated ceramic tiles," *Journal of Photoenergy*, vol. 2012, Article ID 970474, 8 pages, 2012.

[20] Y. Tan, C. Wong, and A. Mohamed, "An overview on the photocatalytic activity of nano-doped-TiO_2 in the degradation of organic pollutants," *Materials Science*, vol. 2011, Article ID 261219, 18 pages, 2011.

[21] D. Verhovšek, N. Veronovski, U. L. štangar, M. Kete, K. žagar, and M. Čeh, "The synthesis of anatase nanoparticles and the preparation of photocatalytically active coatings based on wet chemicalMethods for self-cleaning applications," *International Journal of Photoenergy*, vol. 2012, Article ID 329796, 10 pages, 2012.

[22] H.-X. Tong, Q.-Y. Chen, Z.-L. Yin, H.-P. Hu, D.-X. Wu, and Y.-H. Yang, "Preparation, characterization and photo-catalytic behavior of WO_3-TiO_2 catalysts with oxygen vacancies," *Transactions of Nonferrous Metals Society of China*, vol. 19, no. 6, pp. 1483–1488, 2009.

[23] M. Kim, J. Choi, T. Toops et al., "Coating SiO_2 support with TiO_2 or ZrO_2 and effects on structure and CO oxidation performance of Pt catalyst," *Catalysts*, vol. 3, no. 1, pp. 88–103, 2013.

[24] F. Hussein and A. Halbus, "Rapid decolorization of cobalamin," *International Journal of PhotoenergyInternational Journal of Photoenergy*, vol. 2012, Article ID 495435, 9 pages, 2012.

[25] E. Adamek, W. Baran, J. Ziemianska, and A. Sobczak, "The comparison of photocatalytic degradation and decolorization processes of dyeing effluents," *International Journal of Photoenergy*, vol. 2013, Article ID 578191, 11 pages, 2013.

[26] F. Hussein and T. Abass, "Photocatalytic treatment of textile industrial wastewater," *International Journal of Chemical Sciences*, vol. 8, no. 3, pp. 1353–1364, 2010.

[27] F. Hussein and T. Abass, "Solar photocatalysis and photocatalytic treatment of textile industrial wastewater," *International Journal of Chemical Sciences*, vol. 8, no. 3, pp. 1409–1420, 2010.

[28] F. Hussein, M. Obies, and A. Drea, "Photocatalytic decolorization of bismark brown R by suspension of titanium dioxide," *International Journal of Chemical Sciences*, vol. 8, no. 4, pp. 2736–2746, 2010.

[29] L. Wen, B. Liu, X. Zhao, K. Nakata, T. Murakami, and A. Fujishima, "Synthesis, characterization, and photocatalysis of Fe-doped TiO_2: a combined experimental and Theoretical Study," *International Journal of Photoenergy*, vol. 2012, Article ID 368750, 10 pages, 2012.

[30] M. Shaddad, A. Al-Mayouf, M. Ghanem, M. AlHoshan, J. Singh, and A. Al-Suhybani, "Chemical deposition and electrocatalytic activity of platinum nanoparticles supported on TiO_2 Nanotubes," *International Journal of Electrochemical Science*, vol. 8, pp. 2468–2478, 2013.

[31] L. Ahmed, F. Hussein, and A. Mahdi, "Photocatalytic dehydrogenation of aqueous methanol solution by bare and platinized TiO_2 nanoparticles," *Asian Journal of Chemistry*, vol. 24, no. 12, pp. 5564–5568, 2012.

[32] F. H. Hussein and R. Rudham, "Photocatalytic dehydrogenation of liquid propan-2-ol by platinized anatase and other catalysts," *Journal of the Chemical Society, Faraday Transactions 1: Physical Chemistry in Condensed Phases*, vol. 80, no. 10, pp. 2817–2825, 1984.

[33] F. H. Hussein and R. Rudham, "Photocatalytic dehydrogenation of liquid alcohols by platinized anatase," *Journal of the Chemical Society, Faraday Transactions 1: Physical Chemistry in Condensed Phases*, vol. 83, no. 5, pp. 1631–1639, 1987.

[34] W. Shi, W. Yang, Q. Li, S. Gao, P. Shang, and J. Shang, "The synthesis of nitrogen/sulfur co-doped TiO_2 nanocrystals with a high specific surface areaand a high percentage of 001 facets and their enhanced visible-light photocatalytic performance," *Nanoscale Research Letters*, vol. 7, pp. 1–9, 2012.

[35] V. Štengl and T. M. Grygar, "The simplest way to iodine-doped anatase for photocatalysts activated by visible light," *International Journal of Photoenergy*, vol. 2011, Article ID 685935, 13 pages, 2011.

[36] A. A. Ismail, D. W. Bahnemann, L. Robben, V. Yarovyi, and M. Wark, "Palladium doped porous titania photocatalysts: impact of mesoporous order and crystallinity," *Chemistry of Materials*, vol. 22, no. 1, pp. 108–116, 2010.

[37] K. Cheng, W. Sun, H. Jiang, J. Liu, and J. Lin, "Sonochemical deposition of Au nanoparticles on different facets-dominated anatase TiO_2 single crystals and resulting photocatalytic performance," *The Journal of Physical Chemistry C*, vol. 117, pp. 14600–14607, 2013.

[38] G. Dai, S. Liua, Y. Lianga, H. Liua, and Z. Zhong, "A simple preparation of carbon and nitrogen co-doped nanoscaled TiO_2 with exposed 0 0 1 facets for enhanced visible-light photocatalytic activity," *Journal of Molecular Catalysis A*, vol. 368-369, pp. 38–42, 2013.

[39] S. Liu, J. Yu, and M. Jaroniec, "Tunable photocatalytic selectivity of hollow TiO_2 microspheres composed of anatase polyhedra with exposed 001 facets," *Journal of the American Chemical Society*, vol. 132, no. 34, pp. 11914–11916, 2010.

[40] J. Yu, W. Liu, and H. Yu, "A one-pot approach to hierarchically nanoporous titania hollow microspheres with high photocatalytic activity," *Crystal Growth and Design*, vol. 8, no. 3, pp. 930–934, 2008.

[41] A. H. Lu, E. L. Salabas, and F. Schüth, "Magneticnanoparticles: synthesis, protection, functionalization, and application," *Angewandte Chemie International Edition*, vol. 46, no. 8, pp. 1222–1244, 2007.

[42] T. Nash, "The colorimetric estimation of formaldehyde by means of the Hantzsch reaction," *The Biochemical journal*, vol. 55, no. 3, pp. 416–421, 1953.

[43] C. Castell and B. Smith, "Measurement of formaldehyde in fish muscle using TCA extraction and Nash reagent," *Journal Fisheries Research Board of Canada*, vol. 30, no. 1, pp. 91–98, 1973.

[44] M. Hamadanian, A. Reisi-Vanani, and A. Majedi, "Sol-gel preparation and characterization of Co/TiO_2 nanoparticles: application to the degradation of methyl orange," *Journal of the Iranian Chemical Society*, vol. 7, no. 1, pp. S52–S58, 2010.

[45] J. Cai, J. Huang, H. Yu, and L. Ji, "Synthesis, characterization, and photocatalytic activity of TiO_2 microspheres functionalized with porphyrin," *International Journal of Photoenergy*, vol. 2012, Article ID 348292, 10 pages, 2012.

[46] K. Rahulan, S. Ganesan, and P. Aruna, "Synthesis and optical limiting studies of Au-doped TiO_2 nanoparticles," *Advances in Natural Sciences: Nanoscience and Nanotechnology*, vol. 2, pp. 1–6, 2011.

[47] K. Jackson, "7. A guide to identifying common inorganic fillers and activators using vibrational spectroscopy," *The Internet Journal of Vibrational Spectroscopy*, vol. 3, no. 3, pp. 1–12, 2004.

[48] P. M. Kumar, S. Badrinarayanan, and M. Sastry, "Nanocrystalline TiO_2 studied by optical, FTIR and X-ray photoelectron spectroscopy: correlation to presence of surface states," *Thin Solid Films*, vol. 358, no. 1, pp. 122–130, 2000.

[49] J. J. Murcia, M. C. Hidalgo, J. A. Navío, V. Vaiano, P. Ciambelli, and D. Sannino, "Photocatalytic ethanol oxidative dehydrogenation over Pt/TiO_2: effect of the addition of blue phosphors," *International Journal of Photoenergy*, vol. 2012, Article ID 687262, 2012.

[50] A. Monshi, M. Foroughi, and M. Monshi, "Modified Scherrer equation to estimate more accurately nano-crystallite size using XRD," *World Journal of Nano Science and Engineering*, vol. 2, pp. 154–160, 2012.

[51] D. Moore and R. Reynolds, *X-Ray Diffraction and the Identification and Analysis of Clay Minerals*, Oxford University Press, Oxford, UK, 2nd edition, 1997.

[52] B. Kouakou, L. Ouattara, A. Trokourey, and Y. Bokra, "Characterization of thermal prepared platinized tin dioxide electrodes: application to methanol electro-oxidation," *Journal of Applied Sciences and Environmental Management*, vol. 12, no. 4, pp. 103–110, 2008.

[53] U. M. űller, *Inorganic Structural Chemistry*, John Wiley & Sons Ltd, England, UK, 2nd edition, 2006.

[54] B. Yarmand and S. K. Sadrnezhaad, "Structural and optical properties of Pd^{2+}-doped mesoporous TiO_2 thin films prepared by sol-gel templating technique," *Optoelectronics and Advanced Materials, Rapid Communications*, vol. 4, no. 10, pp. 1572–1577, 2010.

[55] D. Ozkaya, "Particle size analysis of supported platinum catalysts by TEM," *Platinum Metals Review*, vol. 52, no. 1, pp. 61–62, 2008.

[56] X. Pan, I. Medina-Ramirez, R. Mernaugh, and J. Liu, "Nanocharacterization and bactericidal performance of silver modified titania photocatalyst," *Colloids and Surfaces B*, vol. 77, no. 1, pp. 82–89, 2010.

[57] K. Eufinger, D. Poelman, H. Poelman, R. De Gryse, and G. Marin, "TiO_2 thin films for photocatalytic applications," in *Thin Solid Films: Process and Applications*, S. Nam, Ed., pp. 189–227, 2008.

[58] N. Venkatachalam, M. Palanichamy, and V. Murugesan, "Sol-gel preparation and characterization of nanosize TiO_2: its photocatalytic performance," *Materials Chemistry and Physics*, vol. 104, no. 2-3, pp. 454–459, 2007.

[59] Y. Wang, H. Cheng, L. Zhang et al., "The preparation, characterization, photoelectrochemical and photocatalytic properties of lanthanide metal-ion-doped TiO_2 nanoparticles," *Journal of Molecular Catalysis A*, vol. 151, no. 1-2, pp. 205–216, 2000.

[60] A.-W. Xu, Y. Gao, and H.-Q. Liu, "The preparation, characterization, and their photocatalytic activities of rare-earth-doped TiO_2 nanoparticles," *Journal of Catalysis*, vol. 207, no. 2, pp. 151–157, 2002.

[61] B. K. Vijayan, N. M. Dimitrijevic, J. Wu, and K. A. Gray, "The effects of Pt doping on the structure and visible light photoactivity of titania nanotubes," *Journal of Physical Chemistry C*, vol. 114, no. 49, pp. 21262–21269, 2010.

[62] J. Galvez and S. Rodriguez, *Solar Detoxification*, United Nations Educational, Scientific and Cultural Organization, Spine, 1st edition, 2003.

[63] J. S. Jang, P. H. Borse, J. S. Lee et al., "Photocatalytic hydrogen production in water-methanol mixture over iron-doped $CaTiO_3$," *Bulletin of the Korean Chemical Society*, vol. 32, no. 1, pp. 95–99, 2011.

[64] W. Choi, A. Termin, and M. R. Hoffmann, "The role of metal ion dopants in quantum-sized TiO_2: correlation between photoreactivity and charge carrier recombination dynamics," *Journal of Physical Chemistry*, vol. 98, no. 51, pp. 13669–13679, 1994.

[65] L. Wang and T. Egerton, "The effect of transition metal on the optical properties and photoactivity of nanoparticulate titanium dioxide," *Journal of Materials Science Research*, vol. 1, no. 4, pp. 17–27, 2012.

[66] B. Neppolian, H. Jung, and H. Choi, "Photocatalytic degradation of 4-chlorophenol using TiO_2 and Pt-TiO_2 nanoparticles prepared by sol-gel method," *Journal of Advanced Oxidation Technologies*, vol. 10, no. 2, pp. 369–374, 2007.

[67] Q. Xiang, J. Yu, and P. K. Wong, "Quantitative characterization of hydroxyl radicals produced by various photocatalysts," *Journal of Colloid and Interface Science*, vol. 357, no. 1, pp. 163–167, 2011.

[68] Q. Xiang, J. Yu, B. Cheng, and H. C. Ong, "Microwave-hydrothermal preparation and visible-light photoactivity of plasmonic photocatalyst Ag-TiO_2 nanocomposite hollow spheres," *Chemistry: An Asian Journal*, vol. 5, no. 6, pp. 1466–1474, 2010.